

## The Effect of Breakup Channel on the Fusion Reactions of Some Light and Medium Nuclei

<sup>1</sup>Fouad A. Majeed, <sup>2</sup>Khalid H.H. Al Ateah and <sup>2</sup>Malik S. Mehemed

<sup>1</sup>Department of Physics, College of Education for Pure Sciences

<sup>2</sup>Department of Physics, College of Science, University of Babylon, Babylon, Iraq

---

**Abstract:** The effect of coupled-channel calculations on the total fusion cross section  $\sigma_{\text{fus}}$ , the fusion barrier distribution  $D_{\text{fus}}$  and the reaction probability (prob.) for the light systems ( $^6\text{He}+^{209}\text{Bi}$ ,  $^7\text{Li}+^{59}\text{Co}$ ) and the medium system ( $^{46}\text{Ti}+^{64}\text{Ni}$ ). By means of a semiclassical and full quantum mechanical approaches are discussed. The semiclassical approach used in the present research based on the method of the Alder and Winther for Coulomb excitation. The results obtained from our semiclassical and full quantum mechanical calculations are compared with the available experimental data. The semiclassical calculations agrees reasonably with the full quantum mechanical treatment and they were able to reproduce the experimental data in details for the total fusion reaction cross section  $\sigma_{\text{fus}}$ , the fusion barrier distribution  $D_{\text{fus}}$  and the probability of the reaction.

**Key words:** Breakup channel, fusion reactions, fusion barrier distribution, semiclassical, experimental data, mechanical calculations

---

### INTRODUCTION

In recent years, the investigation of the breakup effect of weakly bound nuclei on the fusion process has been an interesting topics (Canto *et al.*, 2006; Keeley *et al.*, 2007; Back *et al.*, 2014). Different process can take place in collisions involving weakly bound nuclei. One is Direct Complete Fusion (DCF). In this case, the whole projectile fuses with the target without breakup. Several processes can occur after the breakup of the weakly bound projectile nucleus. When all the fragments fuse with the target, the process is called Sequential Complete Fusion (SCF). If only part of the fragments fuses with the target nucleus, it is called Incomplete Fusion (ICF). There is also some possibility that none of the fragments is captured by the target. This process is called Non-Capture Breakup (NCBU). Total Fusion (TF) is the sum of direct and sequential Complete Fusion (CF) and of (ICF), (Rangel *et al.*, 2016; Pradhan, 2011; Dasgupta *et al.*, 1999; Gomes *et al.*, 2013; Brandan and Satchler, 1997) in most experiments only (TF) can be measured (Gomes *et al.*, 2013). Light nuclei such as  $^6\text{Li}$ ,  $^7\text{Li}$  and  $^{11}\text{Be}$  with low breakup thresholds are ideal as they have a large breakup probability (compared with the heavy nuclei with the low breakup thresholds) due to the low Coulomb barriers associated with the breakup. The nucleus  $^4\text{He}$  breaks up in to  $^3\text{He}+n$  or  $4\text{He}$  (p, pn)  $^3\text{He}$  with neutron separation energy  $S_n = 20.850$  MeV;  $^6\text{Li}$  breaks up in to

$^4\text{He}+^2\text{H}$  with separation energy  $S_\alpha = 1.48$  MeV and  $^7\text{Li}$  breaks up in to  $4\text{He}+^3\text{H}$  with  $S_\alpha = 2.45$  MeV (Rangel *et al.*, 2016; Gasques *et al.*, 2009; Bildsten *et al.*, 1990). The major aim of fusion reaction studies involving tightly bound stable nuclei over the last four decades has been to produce medium elements and to understand the mechanism of quantum tunneling in complex many-body systems. Further, the analysis of fusion data supplies very useful information about the nuclear interaction at distances corresponding to the outer side of the Coulomb barrier (Canto *et al.*, 2006; Balantekin and Takigawa, 1998). For systems involving weakly bound projectiles we need to consider the coupling to the continuum in order to study the effect of breakup channel for it. For practical purposes, it becomes necessary to approximate the continuum by a finite set of states as in the Continuum. Discretized Coupled-Channels method (CDCC) (Nunes and Thompson, 1998; Alder and Winther, 1975). A semiclassical treatment alternative based on the classical trajectory approximation of Alder and Winther (AW) (Marta *et al.*, 2002) has been proposed by Canto *et al.* (2005) and Majeed and Abdul-Hussien (2016). Very recently Majeed *et al.* (2017) had employed the semiclassical approach to study the effect of the breakup channel using CDCC method on the fusion reaction cross section  $\sigma_{\text{fus}}$  and the fusion barrier distribution  $D_{\text{fus}}$  for  $^6,^7\text{He}$  halo nuclei. Also, Gomes *et al.* (2005) had performed semiclassical coupled-channels calculations in heavy-ion

fusion reaction for the systems  $^{40}\text{Ar}+^{110}\text{Pd}$  and  $^{132}\text{Sn}+^{48}\text{Ca}$ , they proved that the semiclassical approach including the coupling between the elastic channel and the continuum proves to be very successful in describing the total fusion reaction cross section  $\sigma_{\text{fus}}$  and the fusion barrier distribution  $D_{\text{fus}}$  below and above the Coulomb barrier for medium and heavy systems. The aim of the present study is to employ a semiclassical approach based on to Alder and Winther method (AW) (Marta *et al.*, 2002) originally used to treat the Coulomb excitation of nuclei and full quantum mechanical approach. The semiclassical approach has been implemented and coded by Fortran programming language codename (SCF) and the full quantum mechanical codename (CC) which has been used for the calculation of the total fusion cross section  $\sigma_{\text{fus}}$  (mb), the fusion barrier distribution  $D_{\text{fus}}$  (mb/MeV) and the probability of the reaction for the light systems ( $^6\text{He}+^{209}\text{Bi}$ ,  $^7\text{Li}+^{59}\text{Co}$ ) and the medium system ( $^{46}\text{Ti}+^{64}\text{Ni}$ ). The results obtained will be compared with the corresponding available experimental data.

## MATERIALS AND METHODS

**Channels coupled formalism:** When studying the influence of the breakup process on the fusion cross section, many of theoretical aspects must be taken into account. One should include all the different reaction mechanisms related to the breakup and the relative motion of the fragments and their interactions for the occurrence of complete fusion by the boundary conditions used such as the distance where the fusion is decided and the definitions of CF and ICF related to bound and unbound states (Canto *et al.*, 2006; Gomes *et al.*, 2005). Within the CDCC formalism, a set of coupled channel equations are obtained in:

$$i\hbar\dot{a}_{Q'}(t) = \sum_Q \left[ \delta_{Q',Q} V_{\text{opt}}^{Q'} + \langle Q' | \mathbb{V}(T, t) | Q \rangle \right] e^{i(\epsilon_{Q'} - \epsilon_Q)t/\hbar} a_Q \quad (1)$$

We consider a set of coupled channels labeled by calling the corresponding time-dependent probability amplitude and the excitation,  $a_{Q'}(t)$  and  $E_{Q'}$ , respectively. The system Hamiltonian contains complex optical potentials  $V_{\text{opt}}^{(Q)}(r)$  which are diagonal in channel-space, and the channel-coupling interaction  $\mathbb{V}$ . The imaginary parts of the optical potentials account for the loss of flux going into other channels not considered explicitly and the intrinsic states of the system are represented by the vectors  $|Q\rangle$  (Canto *et al.*, 1995; Cardenas *et al.*, 2002). The time-dependent total fusion probability is given by (Canto *et al.*, 1995; Cardenas *et al.*, 2002; Hussein *et al.*, 1993):

$$T_{\text{fus}}(t) = 1 - \sum_{Q'} |a_{Q'}(t)|^2 \quad (2)$$

We get:

$$\frac{dT_{\text{fus}}}{dt} = - \sum_{Q'} \left( a_{Q'}^* \dot{a}_{Q'} + a_{Q'} \dot{a}_{Q'}^* \right) \quad (3)$$

where,  $a_{Q'}^*$  satisfies the complex conjugate of Eq. 1 can be obtained in form (Canto *et al.*, 1995):

$$\frac{dT_{\text{fus}}}{dt} = - \frac{2}{\hbar} \sum_{Q',Q} \text{Im}[\delta_{Q',Q} V_{\text{opt}}^{Q'} + \langle Q' | \mathbb{V}(T, t) | Q \rangle] e^{i(\epsilon_{Q'} - \epsilon_Q)t/\hbar} a_{Q'} a_Q^* \quad (4)$$

Equation 4 leads to a time-dependent of the formula for the fusion cross section (Canto *et al.*, 1995, 2006; Hussein *et al.*, 1993; Hussein *et al.*, 1992):

$$\sigma_{\text{fus}} = - \frac{k}{E} \sum_{i,j} \langle \phi_i^{(+)} | \text{Im}\{H\} | \phi_j^{(+)} \rangle \quad (5)$$

Where:

$H$  = The full Hamiltonian of the system

$\phi_i^{(+)}$  = The exact wave function in channel  $i$

In most applications, the channel-coupling interaction is taken to be real. These equations should be solved with initial conditions  $a_{Q'}(t \rightarrow -\infty) = \delta_{Q',0}$  which means that before the collision ( $t \rightarrow -\infty$ ) the projectile was in its ground state. The final population of channel  $Q$  in a collision with angular momentum  $l$  is  $T_1(Q') = |a_{Q'}(l, t \rightarrow \infty)|^2$  and the cross section is:

$$\sigma_{\text{fus}}^{Q'} = \frac{\pi}{k^2} \sum_{l=0}^{\infty} (2l+1) T_1^{\text{fus}} \quad (6)$$

$$T_1^{\text{fus}} = 1 + \exp \left[ \frac{2\pi}{\hbar W} \left[ B_C + \frac{\hbar^2 l(l+1)}{2\mu R_C^2} - E_{\text{C.m}} \right] \right] \quad (7)$$

where,  $B_C$  and  $R_C$  are the Coulomb Barrier Radius and height, respectively. When incorporating the breakup channel coupling effect (Hussein *et al.*, 1993) where:

$$T_1^{\text{BU}} = 1 - \exp \left[ -2 \int_{\rho_0}^{\infty} \frac{\text{Im} V_{\text{pol}}/E_{\text{c.m}}}{\sqrt{1 - 2\eta/\rho - l(l+1)/\rho^2}} d\rho \right] \quad (8)$$

the dynamic polarization potential is  $V_{\text{pol}}$ , arising from the coupling of the elastic channel to the breakup one.  $\eta$  is the Sommerfeld parameter and  $\rho_0$  is the distance of closest approach, multiplied by the wave number  $k$ , obtained from  $1 - 2\eta/\rho_0 - l(l+1)/\rho_0^2 = 0$ . Then the total breakup probability will be given by Ibraheem and Bonaccors (2005):

$$T_1^{BU}(\text{total}) = T_1^{BU(N)} + T_1^{BU(C)} \quad (9)$$

Where:

$T_1^{BU(N)}$  = The nuclear breakup probability

$T_1^{BU(C)}$  = The Coulomb breakup probability was extensively discussed by Ibraheem and Bonaccors (2005)

The partial fusion probability  $T_1^{\text{fus}}$  has to be multiplied by the breakup survival probability  $(1-T_1^{BU})$  as the fusion cross section is then given by Ibraheem and Bonaccors (2005):

$$\sigma_{\text{fus}}^{O'} = \frac{k}{\pi^2} \sum_{l=0}^{\infty} (2l+1) (1-T_1^{BU}) T_1^{\text{fus}} \quad (10)$$

Since, breakup effects on the fusion cross section are in two types. The first effect is the static effect related with different barrier characteristics when compared with those for similar tightly bound systems: since, the longer tail of the nuclear density of weakly bound nuclei, the static effect enhances the fusion cross section of weakly bound nuclei. The other effect is the dynamical one associated with the strong coupling between the elastic and the breakup channels. When double folding potentials with realistic densities of the colliding nuclei are used as the bare potential, the possible static effects of the weakly bound nuclei are already taken into account, so that, the differences between data and calculations show only the dynamical effects of the channels not included in the calculations. The most reliable calculations related to the breakup process which feeds states in the continuum are the Continuum Discretized Coupled Channel (CDCC) calculations (Gomes *et al.*, 2013).

**Fusion barrier distribution:** The barrier distribution function (Ibraheem and Bonaccors, 2005; Takigawa *et al.*, 2003; Shaikh *et al.*, 2015; Rowley *et al.*, 1991) has developed as an important tool to probe the reaction dynamics of projectile-target collision at energies around the Coulomb barrier (Takigawa *et al.*, 2003). Breakup or breakup like processes, e.g., transfer followed by breakup, competes strongly with the fusion reaction in generating the absorption at low energies. When one of the colliding nuclei is weakly bound. In the last decade, fusion barrier distribution for systems involved weakly bound projectiles have been studied (Shaikh *et al.*, 2015; Rowley *et al.*, 1991). To determine the barrier heights B and the corresponding weights D (B) from fusion cross section is given by the sum of the fusion cross section from distributed fusion barriers in form:

$$\sigma(E) = \int_0^{\infty} \sigma^0(E; B) D(B) dB \quad (11)$$

The barrier position and the corresponding weight can be found by taking the derivative of the barrier transmission probability with respect to energy. By considering a one-dimensional barrier transmission problem (Canto *et al.*, 2005; Dasgupta *et al.*, 1998). By using classical formula of fusion cross section is:

$$\sigma_{\text{fus}}^{(0)}(E) \approx \pi R_B^2 \left( 1 - \frac{V_B}{E} \right) \quad (12)$$

we can prove that barrier distribution as Majeed and Abdul-Hussien (2016), Canto *et al.* (2005), Dasgupta *et al.* (1998), Steadman and Rhoades-Brown (1986):

$$D_{\text{fus}}(E) = \frac{1}{\pi R_B^2} \frac{d^2(E\sigma)}{dE^2} = \frac{1}{\pi R_B^2} \frac{d^2(Q)}{dE^2} \quad (13)$$

the barrier distribution was obtained theoretical from the fusion excitation function by the point difference method is given by:

$$\frac{d^2(Q)_2}{dE^2} = \frac{(Q)_3 + (Q)_1 - 2(Q)_2}{\Delta E^2} \quad (14)$$

the statistical error  $\delta_c$  associated with the second derivative at energy E is approximately given by:

$$\delta_c \cong \frac{E^2}{dE^2} \sqrt{(\rho_{\text{fus}})_1^2 + 4(\rho_{\text{fus}})_2^2 + (\rho_{\text{fus}})_3^2} \quad (15)$$

where,  $\rho$  are the absolute cross section uncertainties. The experimental  $D_{\text{fus}}$  are obtained from apply fitting for the cross section data by using approximate Wong formula which obtain from (Canto *et al.*, 2005; Dasgupta *et al.*, 1998):

$$\sigma_{\text{Wong}} = R_B^2 \frac{\hbar\omega}{2E} \ln \left( 1 + \exp \left\{ \frac{2\pi(E-V)}{\hbar\omega} \right\} \right) \quad (16)$$

## RESULTS AND DISCUSSION

In this study, our theoretical results obtained for the total fusion cross section  $\sigma_{\text{fus}}$ , the fusion barrier distribution  $D_{\text{fus}}$  and the reaction probability (prob.) using the semiclassical approach for the light systems ( $^6\text{He} + ^{209}\text{Bi}$ ,  $^7\text{Li} + ^{59}\text{Co}$ ) and the medium system ( $^{46}\text{Ti} + ^{64}\text{Ni}$ ) are explained. Our calculations results of  $\sigma_{\text{fus}}$ ,  $D_{\text{fus}}$  and (prob.) are compared with the crossponding experimental data and with the full quantum mechanical calculations has been performed by using the code (CC) The Akyuz-Winther potential parameters used in the present calculations are displayed in Table 1.

Table 1: Parameters used in the Akyuz-Winther potential for real and imaginary parts

System	(MeV)	(fm)	(fm)	W(MeV)	(fm)	(fm)
${}^6\text{He}+{}^{209}\text{Bi}$	-123.4	1.130	0.550	-39.3	0.914	0.786
${}^7\text{Li}+{}^{59}\text{Co}$	95.7	1.200	0.500	-30.4	0.915	0.785
${}^{46}\text{Ti}+{}^{64}\text{Ni}$	-142.6	1.080	0.750	-37.6	0.964	0.736

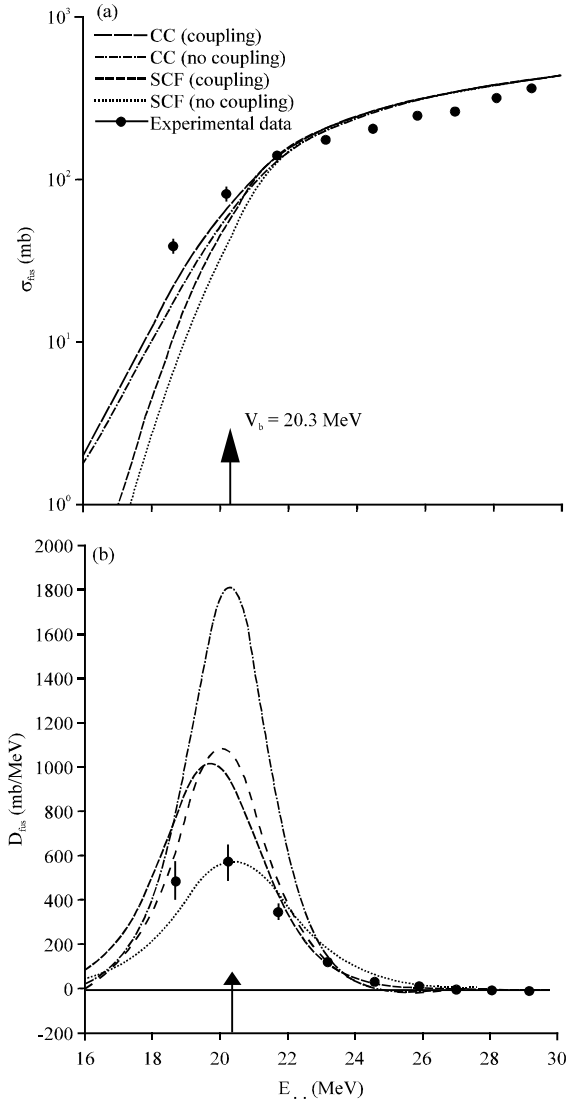


Fig. 1: The comparison between semiclassical (blue curves) and full quantum mechanical (red curves) with the experimental data (green filled circles) for  ${}^6\text{He}+{}^{209}\text{Bi}$  system. Panel: a) For the total fusion cross section  $\sigma_{\text{fus}}$  and b) Panel for the fusion barrier distribution  $D_{\text{fus}}$ . The arrow on the x-axis indicate the position of the Coulomb barrier  $V_b$

**The  ${}^6\text{He}+{}^{209}\text{Bi}$  system:** The calculations of the fusion cross section  $\sigma_{\text{fus}}$  and fusion barrier distribution  $D_{\text{fus}}$  is

presented in Fig. 1 panel a and b, respectively for the system  ${}^6\text{He}+{}^{209}\text{Bi}$ . The dashed blue and red curves represent the semiclassical and full quantum mechanical calculations without coupling, respectively. The solid blue and red curves are the calculations including the coupling effects for the semiclassical and full quantum mechanical calculations, respectively. Panel (a) shows the comparison between our semiclassical and full quantum mechanical calculations with the corresponding experimental data (solid green circles). The experimental data for this system are obtained from Kolata *et al.* (1998).

**Below  $V_b$ :** The best calculated Chi-square value obtained is  $\chi^2 = 0.052212$  for CC as shown in Table 2 which corresponds to the full quantum mechanical calculations with coupled channel calculations including coupling are in best agreement with the experimental data for the total fusion cross section  $\sigma_{\text{fus}}$  below the Coulomb barrier  $V_b$ . For the fusion barrier distribution  $D_{\text{fus}}$  calculations the lowest obtained is  $\chi^2 = 0.007859$  for SCF Code which corresponds to the semiclassical calculations without coupled channel calculations included are in best agreement with the corresponding experimental data. The calculations of probability it is found that the best calculated Chi-square value obtained is  $\chi^2 = 0.008556$  for CC code which corresponds to the full quantum mechanical including channel coupling are in best agreement with the corresponding experimental data as displayed in Table 2.

**Above  $V_b$ :** The best calculated Chi-square value obtained is  $\chi^2 = 0.231016$  for CC Code as shown in Table 2 which corresponds to the full quantum mechanical calculations including coupling are in best agreement with the experimental data for the total fusion cross section  $\sigma_{\text{fus}}$ . For the calculations of the fusion barrier distribution  $D_{\text{fus}}$  the lowest value obtained is  $\chi^2 = 0.004492$  for SCF code and which corresponds to the semiclassical calculations without coupling are in best agreement with the corresponding experimental data. The calculations of probability it is found that the best calculated Chi-square value obtained is  $\chi^2 = 0.006163$  for CC code which corresponds to the full quantum mechanical including channel coupling are in best agreement with the corresponding experimental data as displayed in Table 2 and Fig. 2.

**The  ${}^7\text{Li}+{}^{59}\text{Co}$  system:** Figure 3a, b panel presents the comparison between our theoretical calculations for the total fusion reaction cross section  $\sigma_{\text{fus}}$  and the fusion reaction barrier distribution  $D_{\text{fus}}$  using both semiclassical and quantum mechanical calculations with

Table 2: The obtained Chi-square values from comparison between theory and experiment for the  ${}^6\text{He}+{}^{209}\text{Bi}$  system for the total fusion cross section  $\sigma_{\text{fus}}$  and the fusion barrier distribution  $D_{\text{fus}}$  and the probability above and below the Coulomb barrier  $V_b$

System	CC				SCF			
	Coupling		No coupling		Coupling		No coupling	
	Above $V_b$	Below $V_b$	Above $V_b$	Below $V_b$	Above $V_b$	Below $V_b$	Above $V_b$	Below $V_b$
${}^6\text{He}+{}^{209}\text{Bi}$								
$\sigma_{\text{fus}}$	0.231016	0.052212	0.231625	0.102961	0.294135	0.274534	0.238942	0.669994
$D_{\text{fus}}$	0.011724	0.027715	0.045975	0.098209	0.004857	0.026685	0.004492	0.007859
Prob.	0.006163	0.008556	0.006351	0.012650	0.006999	0.111651	0.009896	0.349463

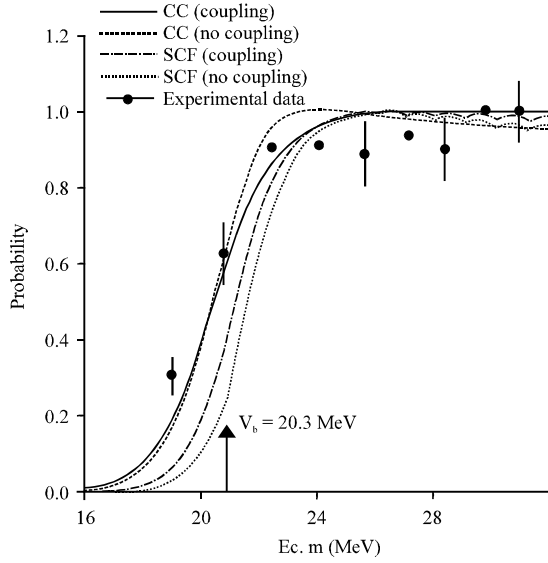


Fig. 2: The comparison between the probability of the reaction for both semiclassical (blue curves) and full quantum mechanical (red curves) with the corresponding experimental data for  ${}^6\text{He}+{}^{209}\text{Bi}$  system

the corresponding experimental data for the system  ${}^7\text{Li}+{}^{59}\text{Co}$  the experimental data for this system are obtained from Beck *et al.* (2003). The dashed blue and red curves represent the semiclassical and full quantum mechanical calculations without coupling, respectively. The solid blue and red curves are the calculations including the coupling effects for the semiclassical and full quantum mechanical calculations, respectively. The calculated Chi-square values for the total fusion cross section, fusion barrier distribution and probability for both semiclassical and quantum mechanical calculations compared to the corresponding experimental data are tabulated in Table 3.

**Below  $V_b$ :** The calculated Chi-square values tabulated in Table 3 are  $\chi^2 = 0.000291$  for CC code in the case of coupling channel calculations which corresponds to full quantum mechanical calculations including coupling are

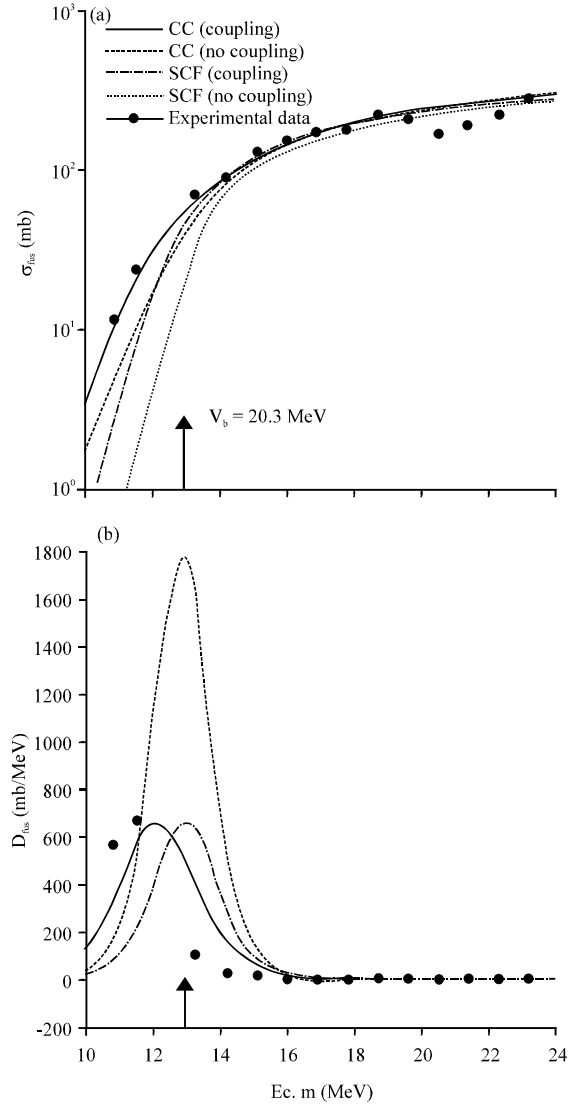


Fig. 3: The comparison between semiclassical (blue curves) and full quantum mechanical (red curves) with the experimental data (green filled circles) for  ${}^7\text{Li}+{}^{59}\text{Co}$  system: a) Panel for the total fusion cross section  $\sigma_{\text{fus}}$  and b) Panel for the fusion barrier distribution  $D_{\text{fus}}$ . The arrow on the x-axis indicate the position of the Coulomb barrier  $V_b$

Table 3: The obtained Chi-square values from comparison between theory and experiment for the  ${}^7\text{Li}+{}^{59}\text{Co}$  system for the total fusion cross section  $\sigma_{\text{fus}}$  and the fusion barrier distribution  $D_{\text{fus}}$  and the probability above and below the Coulomb barrier  $V_b$

System	CC				SCF			
	Coupling		No coupling		Coupling		No coupling	
	Above $V_b$	Below $V_b$	Above $V_b$	Below $V_b$	Above $V_b$	Below $V_b$	Above $V_b$	Below $V_b$
${}^7\text{Li}+{}^{59}\text{Co}$								
$\sigma_{\text{fus}}$	0.021100	0.000291	0.024223	0.009230	0.016785	0.021405	0.036187	0.196454
$D_{\text{fus}}$	0.056239	0.065567	0.215991	0.215991	0.093339	0.138246	0.093339	0.138246
Prob.	0.001069	0.002180	0.002180	0.035544	0.044421	0.049206	0.508431	0.511210

in best agreement with the experimental data for the calculations of the total fusion cross section  $\sigma_{\text{fus}}$ . The best obtained value of Chi-square for the fusion distribution calculations is  $\chi^2 = 0.065567$  for CC code in the case of coupling channel calculations and which correspond the full quantum calculations including coupling effects which means that they are able to reproduce the experimental data better than other calculations. The calculations of probability the best calculated Chi-square value obtained is  $\chi^2 = 0.002180$  for CC code and which corresponds to the full quantum mechanical with coupled channel calculations are in best agreement with the corresponding experimental data.

**Above  $V_b$ :** The calculated Chi-square values tabulated in Table 3 is found to be  $\chi^2 = 0.016785$  for SCF Code in the case of coupling channel calculations and which corresponds to the semiclassical calculations are in best agreement with the experimental data for the calculations of the total fusion cross section  $\sigma_{\text{fus}}$ . The best obtained value of Chi-square for the fusion barrier distribution calculations is  $\chi^2 = 0.056239$  for CC code and which correspond the full quantum mechanical calculations including coupling effects which means that they are able to reproduce the experimental data better than other calculations. The calculations of probability the best obtained Chi-square value is  $\chi^2 = 0.001069$  for CC code which corresponds to the full quantum mechanical with coupled channel calculations are in best agreement with the corresponding experimental data. The full quantum mechanical calculations including coupling are able to reproduce the probability very well as shown in Fig. 3 and 4.

**The  ${}^{46}\text{Ti}+{}^{64}\text{Ni}$  system:** The calculations of the fusion cross section  $\sigma_{\text{fus}}$  and fusion barrier distribution  $D_{\text{fus}}$  is presented in Fig. 5a, b panel, respectively for the system  ${}^{46}\text{Ti}+{}^{64}\text{Ni}$ . The dashed blue and red curves represent the semiclassical and full quantum mechanical calculations without coupling, respectively. The solid blue and red curves are the calculations including the coupling effects for the semiclassical and full quantum

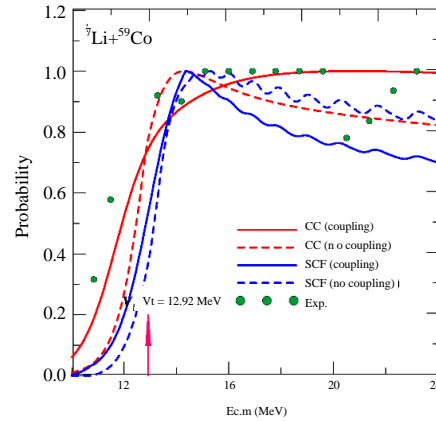


Fig. 4: The comparison between the probability of the reaction for both semiclassical (blue curves) and full quantum mechanical (red curves) with the corresponding experimental data for  ${}^7\text{Li}+{}^{59}\text{Co}$  system

mechanical calculations, respectively. Figure 5a shows the comparison between our semiclassical and full quantum mechanical calculations with the respective experimental data (solid green circles). The experimental data for this system obtained from Prasad *et al.* (1996). The calculated Chi-square values for the total fusion cross section and fusion barrier distribution for both semiclassical and quantum mechanical coupled channel compared with the corresponding experimental data.

**Below  $V_b$**  The best calculated Chi-square value obtained is  $\chi^2 = 0.000555$  for CC code as shown in Table 4 which corresponds to the full quantum mechanical without coupled channel calculations included are in best agreement with the experimental data for the total fusion cross section  $\sigma_{\text{fus}}$ . For the fusion barrier distribution  $D_{\text{fus}}$  calculations the lowest obtained value is  $\chi^2 = 0.001148$  for CC code and which corresponds to the full quantum mechanical calculations with coupled channel calculations are in best agreement with their corresponding experimental data. The calculations of probability the best calculated Chi-square value obtained is  $\chi^2 = 0.000006$  for CC code and which corresponds to the full quantum

Table 4: The obtained Chi-square values from comparison between theory and experiment for the  $^{46}\text{Ti} + ^{64}\text{Ni}$  system for the total fusion cross section  $\sigma_{\text{fus}}$  and the fusion barrier distribution  $D_{\text{fus}}$  and the probability above and below the Coulomb barrier  $V_b$

System	CC				SCF			
	Coupling		No coupling		Coupling		No coupling	
	Above $V_b$	Below $V_b$	Above $V_b$	Below $V_b$	Above $V_b$	Below $V_b$	Above $V_b$	Below $V_b$
$^{46}\text{Ti} + ^{64}\text{Ni}$								
$\sigma_{\text{fus}}$	0.000119	0.000563	0.000110	0.000555	0.161424	0.161696	0.495619	0.496028
$D_{\text{fus}}$	0.001137	0.001148	0.486635	0.488567	0.002417	0.002665	0.005769	0.007591
Prob.	0.000004	0.000006	0.014453	0.014454	0.234173	0.234179	0.926675	0.926678

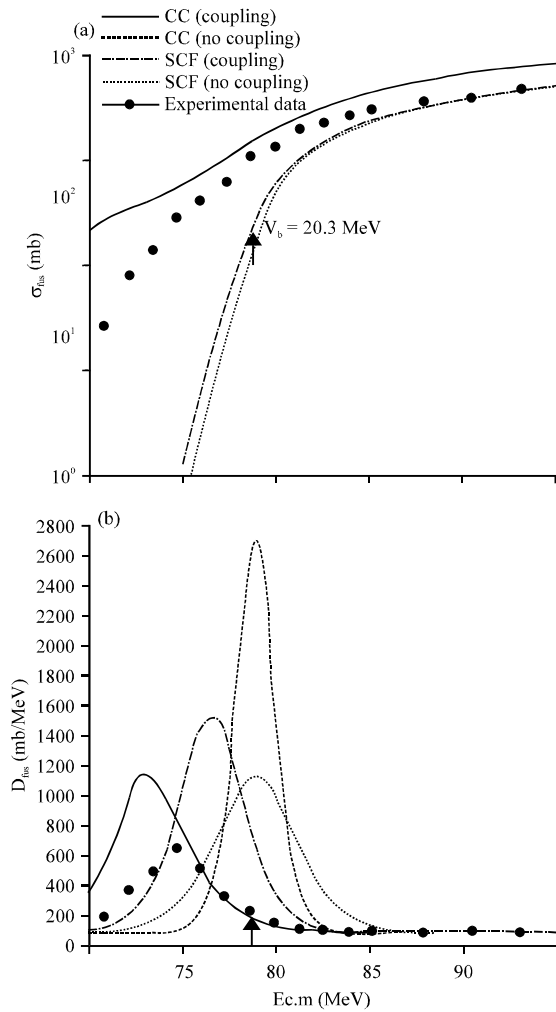


Fig. 5: The comparison between semiclassical (blue curves) and full quantum mechanical (red curves) with the experimental data (green filled circles) for  $^{46}\text{Ti} + ^{64}\text{Ni}$  system: a) Panel for the total fusion cross section  $\sigma_{\text{fus}}$  and b) Panel for the fusion barrier distribution  $D_{\text{fus}}$ . The arrow on the x-axis indicate the position of the Coulomb barrier  $V_b$

mechanical with coupled channel calculations are in best agreement with their corresponding experimental data.

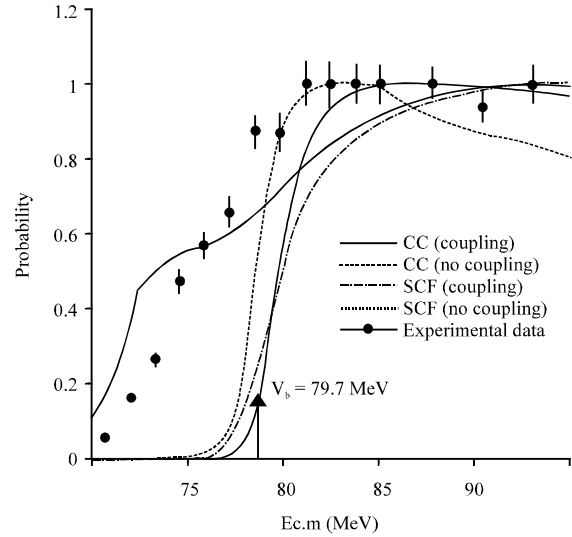


Fig. 6: The comparison between the probability of the reaction for both semiclassical (blue curves) and full quantum mechanical (red curves) with the corresponding experimental data for  $^{46}\text{Ti} + ^{64}\text{Ni}$  system

**Above  $V_b$ :** The best calculated Chi-square value obtained is  $\chi^2 = 0.000110$  for CC code as shown in Table 2 which corresponds to the full quantum mechanical calculations including no coupling are in best agreement with the experimental data for the total fusion cross section  $\sigma_{\text{fus}}$ . For the calculations of the fusion barrier distribution  $D_{\text{fus}}$  the lowest obtained is  $\chi^2 = 0.001137$  for CC code and which corresponds to the full quantum mechanical calculations including coupling are in best agreement with their corresponding experimental data. The calculations of probability the best calculated Chi-square value obtained is  $\chi^2 = 0.000004$  for CC code and which corresponds to the full quantum mechanical with coupled channel calculations are in best agreement with their corresponding experimental data. The full quantum mechanical calculations including coupling are able to reproduce the probability very well as shown in Fig. 6.

## CONCLUSION

The semiclassical approach including the coupling between the elastic channel and the continuum proves to

be very successful in describing the the total fusion cross section  $\sigma_{\text{fus}}$ , the fusion barrier distribution  $D_{\text{fus}}$  and the reaction probability (prob.) for the light systems ( ${}^6\text{He}+{}^{209}\text{Bi}$ ,  ${}^7\text{Li}+{}^{59}\text{Co}$ ) and the medium system ( ${}^4\text{He}+{}^6\text{Ni}$ ). Our theoretical results obtained from semiclassical and full quantum mechanical calculations are compared with the available experimental data. The semiclassical calculations agrees reasonably with the full quantum mechanical treatment and they were able to reproduce the experimental data in details for the total fusion reaction cross section  $\sigma_{\text{fus}}$ , the fusion barrier distribution  $D_{\text{fus}}$  and the probability of the reaction.

## REFERENCES

- Alder, K. and A. Winter, 1975. Electromagnetic Excitation: Theory of Coulomb Excitation with Heavy Ions. North-Holland Publishing Company, Amsterdam, Netherlands, ISBN:9780444108265, Pages: 364.
- Back, B.B., H. Esbensen, C.L. Jiang and K.E. Rehm, 2014. Recent developments in Heavy-ion fusion reactions. *Rev. Mod. Phys.*, 86: 317-360.
- Balantekin, A.B. and N. Takigawa, 1998. Quantum tunneling in nuclear fusion. *Rev. Mod. Phys.*, 70: 1-55.
- Beck, C., F.A. Souza, N. Rowley, S.J. Sanders and N. Aissaoui *et al.*, 2003. Near-barrier fusion of weakly bound  ${}^6\text{Li}$  and  ${}^7\text{Li}$  Nuclei with  ${}^{59}\text{Co}$ . *Phys. Rev. C.*, Vol. 67, 10.1103/PhysRevC.67.054602
- Bildsten, L., I. Wasserman and E.E. Salpeter, 1990. A Semi-classical model for breakup reactions of light Nuclei:  ${}^4\text{He}(\text{p}, \text{pn}){}^3\text{He}$ . *Nucl. Phys. A.*, 516: 77-107.
- Brandan, M.E. and G.R. Satchler, 1997. The interaction between light Heavy-ions and what it tells us. *Phys. Rep.*, 285: 143-243.
- Canto, L.F., P.R.S. Gomes, R. Donangelo and M.S. Hussein, 2006. Fusion and breakup of weakly bound Nuclei. *Phys. Rep.*, 424: 1-111.
- Canto, L.F., R. Donangelo and H.D. Marta, 2005. Upper bounds for fusion processes in collisions of weakly bound Nuclei. *Braz. J. Phys.*, 35: 884-887.
- Canto, L.F., R. Donangelo, P. Lotti and M.S. Hussein, 1995. Effect of Coulomb dipole polarizability of halo Nuclei on their Near-barrier fusion with heavy targets. *Phys. Rev. C.*, 52: R2848-R2850.
- Cardenas, W.H.Z., L.F. Canto, R. Donangelo, M.S. Hussein and J. Lubian *et al.*, 2002. Approximations in fusion and breakup reactions induced by radioactive beams. *Nucl. Phys. A.*, 703: 633-648.
- Dasgupta, M., D.J. Hinde, N. Rowley and A.M. Stefanini, 1998. Measuring barriers to fusion. *Annu. Rev. Nucl. Part. Sci.*, 48: 401-461.
- Dasgupta, M., D.J. Hinde, R.D. Butt, R.M. Anjos and A.C. Berriman *et al.*, 1999. Fusion versus Breakup: Observation of large fusion suppression for  ${}^9\text{Be}+{}^{208}\text{Pb}$ . *Phys. Rev. Lett.*, 82: 1395-1398.
- Gasques, L.R., D.J. Hinde, M. Dasgupta, A. Mukherjee and R.G. Thomas, 2009. Suppression of complete fusion due to breakup in the reactions  ${}^{10,11}\text{B}+{}^{209}\text{Bi}$ . *Phys. Rev. C.*, 79: 034605-1-034605-8.
- Gomes, P.R.S., J.L. Rios, J.R. Borges and D.R. Otomar, 2013. Fusion, breakup and scattering of weakly bound Nuclei at near barrier energies. *Open Nucl. Part. Phys. J.*, 6: 10-15.
- Gomes, P.R.S., M.D. Rodriguez, G.V. Marti, I. Padron and L.C. Chamon *et al.*, 2005. Effect of the breakup on the fusion and elastic scattering of weakly bound projectiles on  ${}^{64}\text{Zn}$ . *Phys. Rev. C.*, 71: 24-24.
- Hussein, M.S., M.P. Pato, L.F. Canto and R. Donangelo, 1992. Near-barrier fusion of  ${}^{11}\text{Li}$  with heavy spherical and deformed targets. *Phys. Rev. C.*, 46: 377-379.
- Hussein, M.S., M.P. Pato, L.F. Canto and R. Donangelo, 1993. Real part of the polarization potential for induced 11 fusion reactions. *Phys. Rev. C.*, 47: 2398-2400.
- Ibraheem, A.A. and A. Bonaccorso, 2005. Coulomb breakup effects on the optical potentials of weakly bound Nuclei. *Nucl. Phys. A.*, 748: 414-432.
- Keeley, N., R. Raabe, N. Alamanos and J.L. Sida, 2007. Fusion and direct reactions of halo Nuclei at energies around the Coulomb barrier. *Prog. Part. Nucl. Phys.*, 59: 579-630.
- Kolata, J.J., V. Guimaraes, D. Peterson, P. Santi and R. White-Stevens *et al.*, 1998. Sub-barrier fusion of  ${}^6\text{He}$  with  ${}^{209}\text{Bi}$ . *Phys. Rev. Lett.*, Vol. 81,
- Majeed, F.A. and Y.A. Abdul-Hussien, 2016. Semiclassical treatment of fusion and breakup processes of  ${}^{6,8}\text{He}$  halo Nuclei. *J. Theor. Appl. Phys.*, 10: 107-112.
- Majeed, F.A., R.S. Hamodi and F.M. Hussian, 2017. Semiclassical coupled channels calculations in Heavy-ion fusion reaction. *Adv. Stud. Theor. Phys.*, 11: 415-427.
- Marta, H.D., L.F. Canto, R. Donangelo and P. Lotti, 2002. Validity of the semiclassical approximation for the breakup of weakly bound Nuclei. *Phys. Rev. C.*, 66: 024605-024605.5.
- Nunes, F.M. and I.J. Thompson, 1998. Nuclear interference effects in 8 B sub-Coulomb breakup. *Phys. Rev. C.*, 57: R2818-R2820.
- Pradhan, M.K., 2011. Influence of projectile breakup on fusion with  ${}^{(159)}\text{Tb}$  target. *DAE. Symp. Nucl. Phys.*, 56: 1172-1173.



- Prasad, N.V.S.V., A.M. Vinodkumar, A.K. Sinha, K.M. Varier and D.L. Sastry *et al.*, 1996. Study of transfer channel coupling and entrance channel effects for the near and Sub-barrier fusion of  $^{46}\text{Ti}+^{64}\text{Ni}$ ,  $^{50}\text{Ti}+^{60}\text{Ni}$  and  $^{19}\text{F}+^{93}\text{Nb}$  systems. Nucl. Phys. A., 603: 176-202.
- Rangel, J., J. Lubian, L.F. Canto and P.R.S. Gomes, 2016. Effect of Coulomb breakup on the elastic cross section of the B 8 Proton-halo projectile on a heavy, Pb 208 target. Phys. Rev.C., Vol. 93, 10.1103/PhysRevC.93.054610
- Rowley, N., G.R. Satchler and P.H. Stelson, 1991. On the distribution of barriers interpretation of Heavy-ion fusion. Phys. Lett. B., 254: 25-29.
- Shaikh, M.M., S. Roy, S. Rajbanshi, M.K. Pradhan and A. Mukherjee *et al.*, 2015. Barrier distribution functions for the system  $^6\text{Li}+^{64}\text{Ni}$  and the effect of channel coupling. Phys. Rev. C., Vol. 91,
- Steadman, S.G. and M.J. Rhoades-Brown, 1986. Sub-barrier fusion reactions. Annu. Rev. Nucl. Part. Sci., 36: 649-681.
- Takigawa, N., T. Masamoto, T. Takehi and T. Rumin, 2003. Heavy ion fusion reactions and tunneling nuclear microscope. J. Korean Phys. Soc., 43: S91-S99.